1989

The Effects of Bandwidth Limiting Tuning Elements on a Synchronously Pumped Mode-Locked Dye Laser

Bahram Zandi
Portland State University

THE EFFECTS OF BANDWIDTH LIMITING TUNING ELEMENTS ON A SYNCHRONOUSLY PUMPED MODE-LOCKED DYE LASER

by

BAHRAM ZANDI

A dissertation submitted in partial fulfillment of the requirements for the degree of

DOCTOR OF PHILOSOPHY
in
ELECTRICAL AND COMPUTER ENGINEERING

Portland State University

TO THE OFFICE OF GRADUATE STUDIES:

The members of the committee approve the dissertation of Bahram Zandi presented May 1, 1989.

[redacted]

Lee W. Casperson, Chairman

[redacted]

Richard D. Morris

[redacted]

Faris Badi'i

[redacted]

Pavel K. Smejtek

APPROVED:

[redacted]

Rolf Schaumann, Head, Department of Electrical Engineering

[redacted]

Bernard Ross, Vice Provost for Graduate Studies

AN ABSTRACT OF THE DISSERTATION OF Bahram Zandi for the Doctor of Philosophy in Electrical and Computer Engineering presented May 1, 1989.

Title: The Effects of Bandwidth Limiting Tuning Elements on a Synchronously Pumped Mode-Locked Dye Laser

APPROVED BY MEMBERS OF THE DISSERTATION COMMITTEE:

Lee W. Casperson, Chairman

Richard D. Morris

Faris Badi'i

Pavel K. Smejtek

In this study an improved description of the bandwidth

AN ABSTRACT OF THE DISSERTATION OF Bahram Zandi for the Doctor of Philosophy in Electrical and Computer Engineering presented May 1, 1989.

Title: The Effects of Bandwidth Limiting Tuning Elements on a Synchronously Pumped Mode-Locked Dye Laser

APPROVED BY MEMBERS OF THE DISSERTATION COMMITTEE:

[redacted]

Lee W. Casperson, Chairman

[redacted]

Richard D. Morris

[redacted]

Faris Badi'i

[redacted]

Pavel K. Smejtek

In this study an improved description of the bandwidth

limiting tuning filters has been introduced into a semiclassical model for a synchronously pumped mode-locked dye laser system. This model is an improvement over the traditional rate equation approach since it has detailed representations of the energy levels, rotational distribution, and coherence effects. The new set of equations has been solved numerically using the best available values for the various parameters, and autocorrelations have been computed for a range of different length detuning and bandwidth limiting elements. In the experiments, an acousto-optically mode-locked argon ion laser is used to synchronously pump a rhodamine 6G dye laser. To study the tuning effects, two and three plate birefringent filters and a tuning wedge have been used. Transmission and bandwidth of these filters have been carefully measured as a function of the length detuning. The autocorrelated pulses have been measured as a function of the length detuning. The experimental pulse shapes agree closely with the theoretical solutions for all values of detuning and filter bandwidth. Through a sensitivity analysis, it is shown how this model can be used to select values for the transmission and the bandwidth of the filter to obtain optimum pulse characteristics.

To my mother and to the memory of my father

ACKNOWLEDGEMENTS

I have had many great teachers to whom I am indebted. I would particularly like to thank my adviser, Professor Lee W. Casperson, who taught me all that I know about lasers. I would also like to thank all my family and friends for their support, especially Karen Nordgren. And finally I would like to thank my colleague Dr. Duncan L. MacFarlane for the valuable discussions we had.

TABLE OF CONTENTS

LIST OF TABLES

TABLE PAGE

LIST OF FIGURES

FIGURE PAGE

FIGURE PAGE

CHAPTER I

INTRODUCTION

Synchronous optical pumping is one of the most popular methods of producing tunable ultrashort pulses, which have many practical applications. The gain of an active medium is modulated at a frequency equal to or a multiple of the round-trip frequency of the laser resonator. The output is a train of pulses, synchronous with the pump pulse, but with much smaller durations. These pulses have numerous applications, including for example, high speed spectroscopy. The output of an actively mode-locked ion laser which is loss modulated is used to pump a dye laser which is thereby actively mode-locked through gain modulation and produces picosecond pulses.

Previous studies of synchronously pumped mode-locked laser systems have used rate equation analyses, which describe temporal changes of the atomic populations and the light energy (or the number of photons), neglecting the phase of the light and the atomic polarization. The first approaches used a two level model [1 - 2], and later studies introduced many level model approaches [3 - 19, 21]. The first semi - classical method was introduced by Casperson in 1983 [20] which is the starting point for this dissertation. To achieve tunability several methods

have been used. Organic dye lasers are popular because of the high repetition frequency of the pulses, stability of amplitude and wide wavelength tuning range due to the wide fluorescence of an organic dye. The dye laser was discovered in 1965 by P. Sorokin and coworkers at the IBM laboratories. With dye lasers, synchronous pumping has been achieved either by a continuous pulse train or by a finite pulse train using argon, krypton, or YAG:Nd^{3+} lasers for the pump. Besides dye lasers, other active media used are: color-center crystal lasers, semiconductor crystal lasers, and lasers utilizing nonlinear optical active media such as optical parametric oscillators and Raman lasers [21]. Also combined systems of synchronously pumped tunable picosecond lasers have been used including: active-passive mode locking, synchronously pumped dye lasers with hard excitation, synchronous lasing of tunable lasers at many frequencies, use of binary mixtures of dye solutions, and synchronously pumped tunable lasers with cavity dumping [21].

This dissertation uses the semiclassical Maxwell-Schrödinger approach which has several advantages over the previous rate equation studies. First, it considers vectors for the electric fields, therefore enabling the inclusion of an anisotropic orientational distribution. Second, it includes the phase memory time of the molecular wave functions and a finite vibrational relaxation time in the lower electronic state of the dye laser transition.

Laser power and temporal characteristics are determined by

the interaction between the light and the atoms under the influence of pumping and relaxation. There are three different approaches in treating the laser theoretically: via rate equations, through a semiclassical theory, or using a full quantum mechanical theory. These three formulations are not independent; the rate equation approach is an approximation to the semiclassical approach, which in turn is an approximation to the quantum mechanical approach. The classical collision picture that is behind the simple rate equation approach yields accurate power and threshold predictions and provides a reasonable model for some nonlinear and time dependent effects. Since the rate equations describe temporal changes of atomic populations and light energy or the number of photons, neglecting the phase of the light and atomic polarization, they break down when ensemble effects become important. At the other extreme is the quantum mechanical approach. In the full quantum mechanical theory, both the atoms and the light are quantized and treated quantum mechanically using density matrices [22]. The quantum mechanical approach is typically used when the problem involves quantum noise since it rigorously treats spontaneous emission. It is also essential in answering questions of photon statistics and field buildup from vacuum. A disadvantage of this treatment is that it is too cumbersome.

In the semiclassical theory light is treated as classical electromagnetic waves described by Maxwell equations, while the ensemble of atoms that interact with the electromagnetic field

are described quantum mechanically. Semiclassical effects form a middle ground between the simple rate equation picture and the extensive quantum mechanical theory. Semiclassical theory must be used to describe certain "coherent" interactions between light and matter such as photon echoes, self induced transparency, or spontaneous pulsations from Xe lasers. These effects are really the macroscopic manifestations of a quantum mechanical ensemble and the distribution of information, or "coherence" of that ensemble is inherent in those phenomena.

These coherence effects typically manifest themselves on short time scales. One can probably neglect coherence effects if the intensity changes on a time scale that is long with respect to the coherence time. Since the mode-locked laser pulses studied in this work are only a few picoseconds long and the coherence time of the dye laser medium is 5×10^{-14} sec., it is important to include these coherent effects. Few studies of mode-locked lasers, however, are complete enough to include those effects.

Conversely, we are interested more in the shape of the ideal steady state pulse and not in its buildup from noise. Consequently, in this study we adopt the semiclassical approach and consider the model of a synchronously pumped mode-locked dye laser system with an intracavity tuning element.

The order for the organisation of the chapters is as following: In Chapter II, we present the derivation of our model for a synchronously pumped mode-locked dye laser with a

bandwidth limiting tuning element. Chapter III describes the design of our experiments. Chapter IV deals with our results and conclusions. Chapter V has further numerical studies and sensitivity analysis.

CHAPTER II

THEORY

THE SEMICLASSICAL APPROACH

We now detail further, the components of a semiclassical theory. A semiclassical treatment does not use the quantized radiation field but treats the electromagnetic field as a classical, external force acting on the atomic system providing the gain mechanism. The radiation field induces an electric dipole moment in the material which in turn is used in the classical Maxwell equations to calculate the effect of the gain medium on the field.

A classical electromagnetic field is governed by Maxwell's equations. We demand that the field be self-consistent: the field E that induces the polarization of the active medium must be equal to the resulting field E'. The self consistent loop of the semiclassical formalism is as follows:

E(r , t)→Quantum Mechanics→Statistical Summation→P(r , t)→Maxwell's Equations→E'(r,t)

Here the field induces electric-dipole moments in the medium

according to the laws of quantum mechanics. The density matrix is used to facilitate the statistical summations that govern the interaction of a single particle with an externally applied electric field involved in obtaining the macroscopic polarization of the medium for the individual dipole moments. The density matrix formalism is an extension of quantum mechanics which includes statistical ensemble averaging of incompletely known physical systems. The macroscopic polarization then becomes the driving force in the Maxwell wave equation that produces the field.

In the following sections, we present the derivation of our model for a synchronously pumped mode-locked dye laser with a bandwidth limiting tuning element.

DERIVATION OF THE INHOMOGENEOUS WAVE EQUATION

Starting from the classical Maxwell equations:

$$\nabla \times H = \partial D/\partial t + J \qquad (1)$$

$$\nabla \times E = -\partial B/\partial t \qquad (2)$$

$$\nabla \cdot B = 0 \qquad (1)'$$

$$\nabla \cdot D = \rho \qquad (2)'$$

where E is the electric field, D is the electric flux density (displacement), H is the magnetic field, B is the magnetic flux density, J is the electric current density, and ρ is the charge

density. For the displacement vector **D** we have:

$$\mathbf{D} = e_0\mathbf{E} + \mathbf{P} \qquad (3)$$

where **P** is the polarization vector that represents the material interaction that will be the topic of section c. In the absence of magnetic polarization we have for the magnetic induction vector:

$$\mathbf{B} = \mu_0\,\mathbf{H} \qquad (4)$$

Using the constitutive relations (3) and (4), we can write Maxwell's equations as:

$$\nabla \times \mathbf{H} = e_0\,\delta\mathbf{E}/\delta t + \delta\mathbf{P}/\delta t \qquad (5)$$

$$\nabla \times \mathbf{E} = -\mu_0\,\delta\mathbf{H}/\delta t \qquad (6)$$

Taking the curl of eq.(6) and using eq.(5) we obtain:

$$\nabla \times (\nabla \times \mathbf{E}) = -e_0\mu_0\delta^2\mathbf{E}/\delta t^2 - \mu_0\delta^2\mathbf{P}/\delta t^2 - \mu_0\sigma\delta\mathbf{E}/\delta t \qquad (7)$$

Using the vector identity:

$$\nabla \times (\nabla \times \mathbf{E}) = \nabla(\nabla \cdot \mathbf{E}) - \nabla^2\,\mathbf{E} \qquad (8)$$

and by considering the charge free limit, $\nabla \cdot \mathbf{E} = 0$, we obtain an

inhomogeneous wave equation for the electric field vector

$$\nabla^2 \mathbf{E} - e_0\mu_0 \partial^2\mathbf{E}/\partial t^2 - \mu_0\sigma \partial\mathbf{E}/\partial t = \mu_0 \partial^2\mathbf{P}/\partial t^2 \qquad (9)$$

This equation will give us the field E once we know the polarization P, and may be viewed as complementary to the Schrödinger equation.

Now we assume a plane wave solution for our signal field in the z direction:

$$E_S(z,t) = 1/2\ E_S(z,t)\ \exp[i(k_S z - \omega_S t)] + c.c.$$

Recall that the polarization vector P must be obtained from the quantum theory of the atomic system. This then is our next task.

QUANTUM MECHANICAL DERIVATION OF THE POLARIZATION

The macroscopic polarization has its origin in the microscopic response of a molecule bathed in an electric field [Debye]. We chose to treat this problem in a quantum mechanical framework and thus recall the time dependent Schrödinger equation which may be written as:

$$H\Psi(r,t) = i\hbar\, \partial\Psi(r,t) / \partial t \qquad (10)$$

where H is the Hamiltonian operator,

$$H = -\hbar^2/2m\ \nabla^2 + V(r,E) \qquad (11)$$

Here V is the potential energy of the particle's immediate environment plus a perturbation due to the field.

From the works of Lamb [22], we may now assume a solution form or a sum of orthonormal solutions:

$$\Psi(r,t) = \Sigma\ c_n(t)u_n(r) \qquad (13)$$

Here $u_n(r)$ are solutions to the time independent, unperturbed Schrödinger wave equation. Also using ensemble averaging and introducing the density matrix:

$$\rho_{nm} = c_m^* c_n \qquad (14)$$

we obtain:

$$\delta\rho_{nm}/\delta t = i/\hbar\ \Sigma(\rho_{nj}H_{mj}^* - \rho_{jm}H_{nj}) \qquad (15)$$

or, introducing the commutator notation

$$\delta\rho/\delta t = i/\hbar\ [\rho,H] \qquad (16)$$

Equation (16) is the equation of motion for the density matrix. It relates the time rate of change of the density

matrix element to a Hamiltonian, which for our problem is:

$$H = H_0 + H' = H_0 - \mu E(t)$$

Here, H' is the time dependent perturbation that the molecule feels when subjected to an electric field E(t). The strength of this perturbation is proportional to the dipole moment operator μ, which in turn is proportional to the charge per volume e,

$$\mu = er \qquad (17)$$

Our goal is the macroscopic polarization of equation (9), which we define as the dipole moment per unit volume,

$$P = N \langle \mu \rangle \qquad (19)$$

where N is the number of atoms per volume and $\langle\mu\rangle$ is the expectation value of the dipole moment.

For a two level atomic energy system, we can write the set of density matrix equations as [23]:

$$\delta\rho_{21}/\delta t = -i\omega_0\rho_{21} - i/\hbar\, \mu_{21} \cdot E(\rho_{22} - \rho_{11}) \qquad (21)$$

$$\rho_{12} = \rho_{21}^* \qquad (22)$$

$$d/dt\, (\rho_{22} - \rho_{11}) =$$

$$= -2iE/\hbar\,(\mu_{12}\rho_{21} - \mu_{21}\rho_{12}) \qquad (23)$$

Coherent equations (21-23) represent the stimulated (emission and absorption) response of the atom to an applied, time dependent field. Equation (23) governs the population difference while equations (21) and (22) determine the polarization.

Following from [20], we consider a four level model for our dye laser system as in Figure 1. When the dye is excited by an external source of light, it emits radiation at longer wavelength (fluoresces), absorbing a photon at the excitation wavelength and emitting a photon at the fluorescense wavelength. The energy difference between the absorbed and emitted photon is accounted for by a nonradiative transition in the dye which transforms into heat.

Therefore we can write the density matrix equations for this four level atomic energy system as:

$$\delta\rho_{00}/\delta t = -i/\hbar\,(\rho_{03}\mu_{30} - \rho_{30}\mu_{03}) \cdot E_p + \rho_{11}/\tau_1$$

$$\delta\rho_{33}/\delta t = i/\hbar\,(\rho_{03}\mu_{30} - \rho_{30}\mu_{03}) \cdot E_p - \rho_{33}/\tau_3$$

$$\delta\rho_{22}/\delta t = -i/\hbar\,(\rho_{21}\mu_{12} - \rho_{12}\mu_{21}) \cdot E_s - \rho_{22}/\tau_2 + \rho_{33}/\tau_3$$

$$\delta\rho_{11}/\delta t = i/\hbar\,(\rho_{21}\mu_{12} - \rho_{12}\mu_{21}) \cdot E_s - \rho_{11}/\tau_1 + \rho_{22}/\tau_2$$

$$\delta\rho_{30}/\delta t = -i\omega_{p0}\rho_{30} + i/\hbar\,(\rho_{00} - \rho_{33})\,\mu_{30} \cdot E_p - \rho_{30}/T_p$$

$$\delta\rho_{21}/\delta t = -i\omega_{s0}\rho_{21} - i/\hbar\,(\rho_{22}-\rho_{11})\,\mu_{21}\cdot E_s - \rho_{21}/T_s$$

$$\rho_{03} = \rho_{30}^*$$

$$\rho_{12} = \rho_{21}^*$$

The E_p and E_s are the pump and signal electric fields, ω_{p0} and ω_{s0} are the center frequencies of the pump and signal transitions, T_p and T_s are the coherence times of the off diagonal matrix elements and the μ's are the matrix elements of the dipole moment operator. Note also that we have phenomenologically included the spontaneous decay in terms of the lifetimes τ_1,τ_2,τ_3.

Thus our semiclassical model for a dye laser medium without a filter, consists of three density matrix equations:

$$\delta\rho_{22}/\delta t = \eta_s E_s x/\hbar - \rho_{22}/\tau_2 + T_p|\mu_p|^2 E_p^2 x^2/2\hbar^2 \qquad (25)$$

$$\delta\rho_{11}/\delta t = -\eta_s E_s x/\hbar - \rho_{11}/\tau_1 + \rho_{22}/\tau_2 \qquad (26)$$

$$\delta\eta_s/dt = i(\omega_s-\omega_{s0})\eta_s - (\rho_{22}-\rho_{11})|\mu_s|^2 E_s x - \eta_s/T_s \qquad (27)$$

and one Maxwell equation for the electric field. In section (c) we derived the wave equation and suggested a plane wave

solution. Now we substitute the polarization:

$$P_S = \int n(\theta,\phi)(\rho_{21}\mu_{12} + \rho_{12}\mu_{21})d\Omega$$

with the propagation constant:

$$k_S^2 = \mu e \omega_S^2$$

and phase velocity:

$$v = (\mu e)^{-1/2}$$

and where higher order space and time derivatives of slowly varying quantities are neglected. Also we have used the rotating wave approximation which limits the overall response of the atom to one near resonance. Therefore we obtain:

$$\delta E_S/\delta z + 1/v\ \delta E_S/\delta t + \alpha/2\ E_\sigma = -\ \mu\omega_S^2 N/k_S \int \eta_S x dx \qquad (28)$$

where the ρ 's are population, E_p is the pump field, E_S is the signal field, T_S is the coherence time, μ is the dipole moment, ω is the signal frequency and α is the loss term. Also we have introduced:

$$\eta(\theta,\phi,z,t) = \rho\mu \qquad (29)$$

θ measures the angle of a class of pump dipoles with respect to the z axis.

$x = \cos\theta$, is the molecular distribution factor. It has been shown that the inclusion of x is necessary for a rigorous analysis and for better agreement with the experiment [20]. For unidirectional distribution we can assume:

$$x = 1 \qquad (30)$$

The limit of $T_g = 0$, represents the rate equations approximation.

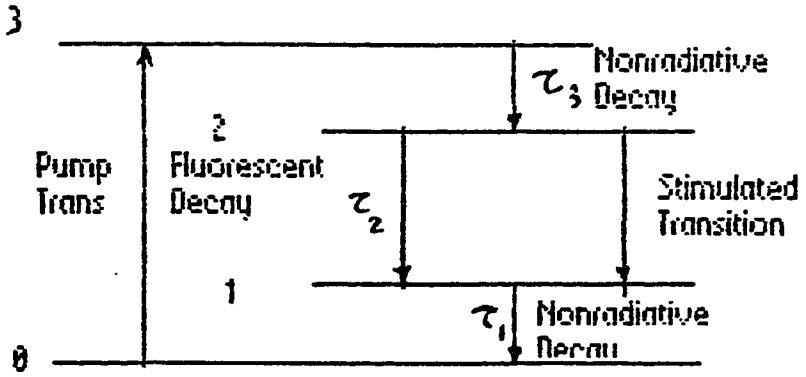

Figure 1. Energy levels of the dye laser model.

INCLUSION OF THE BANDWIDTH LIMITING ELEMENT

To incorporate the bandwidth limiting filter in our dye laser model, we assume that the filter is a two level negative absorber (amplifier), consisting of a bandwidth limiter and an attenuator, and in analogy to real atomic transitions, it has a Lorentzian lineshape (see Figure 2). In a block diagram, using analog elements, we can show it as a linear bandpass filter.

Since for the filter, we assume a two level model, therefore the same dye laser equations (25-28) can be adapted with:

$$\mathbf{E}_p = 0$$

and

$$\tau_1 \to \infty$$

$$\delta\rho_{22f}/\delta t = \boldsymbol{\eta}_f/\hbar\, \mathbf{E}_s - \rho_{22f}/\tau_f \qquad (31)$$

$$\delta\rho_{11f}/\delta t = -\boldsymbol{\eta}_f/\hbar\, \mathbf{E}_s + \rho_{22f}/\tau_f \qquad (32)$$

$$\delta\boldsymbol{\eta}_f/\delta t = i(\omega_s-\omega_{f0})\boldsymbol{\eta}_f - \boldsymbol{\eta}_f/\tau_f - i(\rho_{22f}-\rho_{11f})|\boldsymbol{\mu}_f|^2\mathbf{E}_s/2\hbar \qquad (33)$$

where the subscript f is for the filter. We note that eq. 31 and 32 are not linearly independent, specifically,

$$\delta\rho_{11f}/\delta t = -\delta\rho_{22f}/\delta t \qquad (34)$$

or:

$$\delta(\rho_{11f} + \rho_{22f})/\delta t = 0 \qquad (35)$$

$$\rho_{11f} + \rho_{22f} = \text{constant} \qquad (36)$$

where the arbitrary constant of integration in eq. (36) is chosen to be unity in keeping with the probabilistic interpretation of the density matrix.

Dividing η_f into real and imaginary parts, we have:

$$\eta_f = \eta'_f + i\eta''_f \qquad (37)$$

substituting into eq. (36) we have:

$$\delta\eta'_f/\delta t = -\eta''_f\,(\omega_s - \omega_{f0}) - \eta'_f/\tau_f \qquad (38)$$

$$\delta\eta''_f/\delta t = \eta'_f(\omega_s - \omega_{f0}) - \eta''_f/\tau_f - |\mu_f|^2 E_s(2\rho_{22f} - 1)/2\hbar \qquad (38)$$

To solve for the frequency lineshape for the response of the atoms in steady state, we equate the time derivatives to zero. From eq. (31):

$$\rho_{22f} = \tau E_s \eta''_f / \hbar \qquad (40)$$

From eq. (38):

$$\eta''_f = - \eta'_f / T_f(\omega_s - \omega_{f0}) \qquad (41)$$

From eq. (39):

$$\eta'_f(\omega_s - \omega_{f0}) =$$

$$= - \eta'_f / T_f^2(\omega_s - \omega_{f0}) + |\mu_f|^2 E_s / 2K \left[- 2E_s \tau_f \eta'_f / K T_f(\omega_s - \omega_{f0}) - 1 \right] \qquad (42)$$

solving for η'_f:

$$\eta'_f =$$

$$= - E_s |\mu_f|^2 / 2K \; T_f^2(\omega_s - \omega_{f0}) / [1 + T_f^2(\omega_s - \omega_{f0})^2 + |\mu_f|^2 E_s^2 T_f \tau_f / K^2] \qquad (43)$$

Similarly:

$$\eta''_f =$$

$$= E_s |\mu_f|^2 T_f / 2K [1 + T_f^2(\omega_s - \omega_{f0})^2 + |\mu_f|^2 E_s^2 T_f \tau_f / K^2] \qquad (44)$$

and from (40):

$$\rho_{22f} =$$

$$= \tau_f E_s^2 T_f |\omega_f|^2 / 2K^2 [1 + T_a^2(\omega_s - \omega_{f0})^2 + |\mu_f|^2 E_s^2 T_f \tau_f / K^2] \qquad (45)$$

Now we have a <u>saturating Lorentzian</u>. But a linear filter does not saturate, therefore to have nonsaturating linear filter,

we need to have:

$\tau_f \to 0$ which leads to $\rho_{22} << \frac{1}{2}$

Therefore our equations (31), (38) and (39) become:

$$\delta\rho_{22f}/\delta t = \eta''_f/\hbar\, E_s - \rho_{22f}/\tau_f \qquad (46)$$

$$\delta\eta'_f/\delta t = -\eta''_f(\omega_s-\omega_{f0}) - \eta'_f/T_f \qquad (47)$$

$$\delta\eta''_f/\delta t = \eta'_f(\omega_s-\omega_{f0}) - \eta''_f/T_f + |\mu_f|^2 E_s/2\hbar \qquad (48)$$

Solving for steady state we obtain:

$$\rho_{22f} = \tau_f(E_s/\hbar)\,\eta''_f \qquad (49)$$

$$\eta''_f = -\eta'_f/T_f(\omega_s-\omega_{f0}) \qquad (50)$$

Thus,

$$\eta'_f = $$
$$= |\mu_f|^2 E_s T_f^2(\omega_s-\omega_{f0})/2\hbar[1+T_f^2(\omega_s-\omega_{f0})^2] \qquad (51)$$

$$\eta''_f = $$
$$= |\mu_f|^2 E_s T_f/2\hbar[1+T_f^2(\omega_s-\omega_{f0})^2] \qquad (52)$$

$$\rho_{22f} = $$
$$= |\mu_f|^2 E_s^2 T_f \tau_f/2\hbar^2[1+T_f^2(\omega_s-\omega_{f0})^2] \qquad (53)$$

In equation (52), we observe the unsaturating Lorentzian lineshape.

Since we are interested in the temporal response of the filter at line center we set:

$$\omega_s = \omega_{f0} \qquad (54)$$

then,

$$\eta'_f = 0 \qquad (55)$$

and our filter response equation becomes:

$$\delta\eta''_f/\delta t = -\eta''_f/T_f + |\omega_f|^2 E_s/2\kappa \qquad (56)$$

Equation (56) is the only relevent equation from this set, because the field can only interact with η''_f and ρ_{22f} is decoupled from this equation. We note that eq. (48) is the same equation as eq. (56).

To couple η_h into the field equation for our model, we need to define the parameters characterising our filter amplifier and attenuator. As they are presented in Figure 2, we have shown our bandwidth limiting filter in two parts: First, as an amplifier (absorber) and second, as an attenuator. This formalism is restrictive. We need to select as many parameters for our model of the filter as possible, while keeping efficiency. There are three significant parameters:

1. Bandwidth of the filter at fullwidth half maximum.
2. Maximum transmission of the filter.
3. Minimum transmission of the filter.

From Figure 2, for linewidth correction due to finite interaction length, we have:

Amplifier gain = T_{max}/T_{min}

Attenuator gain = T_{min}

$$I_{out} = I_{in}\, e^{gz}$$

$$I_{out}-I_{in} = I_{in}(e^{gz}-1) \qquad (57)$$

$$e^{g(0)z} = T_{max}/T_{min}$$

$$g(0)z = \ln (T_{max}/T_{min}) \qquad (58)$$

We demand that the difference (57) drop to 1/2. Therefore:

$$1/2 = [e^{g(y_{½})z}-1] \; / \; [e^{g(0)z}-1] \qquad (58\text{-a})$$

According to reference [24] on Spectral Narrowing in High - Gain Lasers, y is the normalized frequency in homogeneously (Doppler) broadened medium and is shown as:

$$y = 2(\nu-\nu_0)/\Delta\nu_h \qquad (58\text{-b})$$

For homogeneous broadening we assume a Lorentzian response:

$$g(y) = g(0) \; / \; [1+y^2]$$

Substituting in (58-a):

$$1/2 = [e^{g(0)z/1+y_{½}^2} - 1] \; / \; [e^{g(0)z} - 1] \qquad (58\text{-c})$$

Then solving for $y_{½}$ in (58-c), we can find $\Delta\nu$ from (58-b):

$$\Delta\nu = \Delta\nu_h[(g(0)z/\ln(e^{g(0)z+1})-\ln 2) \; -1)]^{½}$$

Therefore for the filter bandwidth we have:

$$\Delta\nu_f =$$

$$= \Delta\nu_{trans.\ peak} / [(g(0)z / \ln(e^{g(0)z}+1) - \ln 2)-1]^{\frac{1}{2}}$$

To determine the rest of the parameters we make the following assumptions and find the respective loss factor α for each section of our system:

1. Equal length distribution, that is the length of the dye amplifier is equal to the length of the filter amplifier:

$$z = l_a$$

2. Distributed loss over l_a (smeared):

$$I_2 = T_{min}I_1 = I_1 \exp(-\alpha_f l_a)$$

$$\ln (T_{min}) = -\alpha_f l_a$$

The filter loss factor, α_f would be:

$$\alpha_f = -[\ln (T_{min})] / l_a$$

3. Smeared mirrors:

$$I_2 = R_1R_2I_1 =$$

$$= I_1 \exp(-2\alpha_m l_a)$$

and the mirror loss factor, α_m is:

$$\alpha_m = -[\ln(R_1R_2)] \; / \; 2l_a$$

Therefore the total loss factor α becomes:

$$\alpha = \alpha_s + \alpha_f + \alpha_m =$$

$$= \alpha_s - [\ln (T_{min})] \; / \; l - [\ln (R_1R_2) \; / \; 2l]$$

where α_s is the loss due to the dye jet.

With these corrections, then we can couple η_f into the field equation by extending the atomic analogy. Therefore the final set of equations governing the laser amplifier and the filter is:

$$\delta\rho_{22}/\delta t =$$

$$= \eta'_s E_s x/\hbar - \rho_{22}/\tau_2 + T_p|\mu_p|^2 E_p^2 x^2/2\hbar^2 \qquad (59\text{-a})$$

$$\delta\rho_{11}/\delta t =$$

$$= -\eta'_s E_s x/\hbar - \rho_{11}/\tau 1 + \rho_{22}/\tau 2 \qquad (59\text{-b})$$

$$\delta\bar{n}_s/\delta t =$$

$$= -(\rho_{22}-\rho_{11})|\mu_s|^2 E_s x - \eta'_s/T_s \qquad (59\text{-c})$$

$$\delta\eta'_f/\delta t =$$

$$= -d|\mu_f|^2 E_s - \eta'_f/T_f \qquad (59\text{-d})$$

$$\delta E_s/\delta z + 1/v\ \delta E_s/\delta t =$$

$$= -\alpha_s E_s/2 - \mu\omega_s^2 N/k_s \int \eta'_s x dx - \mu\omega_s^2 N_f \eta'_f/k_s - \alpha_f E_s/2 - \alpha_m E_s/2 \qquad (59\text{-}e)$$

where d is the strength of the unsaturating amplifier and the α's are the loss terms.

THE STEADY STATE LIMIT AND NORMALIZATION

The steady state solution is useful because it suggests a normalization. To study the filter effect by itself on the EM field, we set all the time derivatives equal to zero and solve for the E's response:

From eq. (59-c):

$$\delta \eta_s/\delta t = 0$$

$$\eta_s = (\rho_{22}-\rho_{11}) E_s \,/\, [1 + (\mu_s)^2 \tau_2 T_s E_s^2/\hbar^2] \qquad (59\text{-}f)$$

From eq. (59-d):

$$\eta'_f = -dT_f |\mu_f|^2 E_s \,/\, 2\hbar$$

and from the field eq. (59-e):

$$\delta E_s/\delta z + \alpha_a E_s/2 = \mu\omega_s^2 N_f d T_f |\mu_f|^2 E_s/2k_s\hbar = g_f(0)E_s/2$$

By introducing suitable normalized forms for the dependent variables, we can write our set of equations in a more compact form. We normalize the field in the form of a parameter called A to become equal to 1 for when the steady state gain drops to 1/2 its small signal value, as per eq. (59-f)

$$A = |\mu_s|/\hbar\ (\tau_2 T_s/2)^{1/2} E_s$$

$$D = \mu\omega_s^2 N T_s |\mu_s|^2 (\rho_{22}-\rho_{11})/k_s\hbar\alpha$$

$$M = \mu\omega_s^2 N T_s |\mu_s|^2 (\rho_{22}+\rho_{11})/k_s\hbar\alpha$$

$$Q = -\mu\omega_s^2 N |\mu_s| (2\tau_2 T_s)^{1/2} \eta'_s/k_s\hbar\alpha$$

$$P = \mu\omega_s^2 N T_s |\mu_s|^2 \tau_2 T_p |\mu_p|^2 E_p^2/2k_s\alpha\hbar^3$$

$$F = -2\hbar |\mu_s| \tau_2 T_s \eta'_f/2T_f d |\mu_f|^2\hbar$$

Here, D is the normalized population difference, M is the normalized population sum, Q is the normalized polarization, P is the normalized pump rate, F is the normalized filter response, and A is the normalized field. With these new variables, our set of equations becomes:

$$\delta D/\delta t =$$

$$-1/\tau_2[(1+\tau_2/2\tau_1)D+(1-\tau_2/2\tau_2)M+2QAx-P(\tau)x^2] \qquad (60\text{-a})$$

$$\delta M/\delta t =$$

$$-1/\tau_2(\tau_2/2\tau_1 D+\tau_2/2\tau_1 M-P(\tau)x^2) \qquad (60\text{-b})$$

$$\delta Q/\delta t = -(Q - ADx) / T_s \qquad (60\text{-c})$$

$$\delta F/\delta t = -(F - A) / T_f \qquad (60\text{-d})$$

$$\delta A/\delta z + 1/v\ \delta A/\delta t = -\alpha/2\ (A - \int Qxdx - g_f F/\alpha) \qquad (60\text{-e})$$

SYNCHRONOUS PUMPING

Now we take account of the timing consideration imposed by synchronous pumping by including them in a boundary condition. Smearing the length of the dye jet l_a in the single path length of the dye laser cavity, L. The last equation can be written:

$$\delta A/\delta z + 1/v\ \delta A/\delta t =$$

$$= -\alpha/2\ (A - \int Qxdx - g_f F/\alpha)(l_a/L_d ye) \qquad (61)$$

Introducing a new time coordinate:

$$\tau = t - z/v_s$$

where v_s is the envelope speed for the steady state pulse in the dye. Imposing a steady state pulse requirement, our set of equations change from partial differential equations to ordinary differential equations. Accordingly, the field equation (61) becomes:

$$dA/d\tau =$$

$$= -v\alpha/2(1 - v/v_s)(1 / L_{dye})(A - \int Qxdx - g_f lF/\alpha_l) \qquad (62)$$

where α is the sum of all the losses:

$$\alpha =$$

$$\alpha_s + \alpha_f + \alpha_m =$$

$$= \alpha_s - \ln (T_{min}/1) - \ln (R_1R_2/21)$$

and from:

$$e^{-2\alpha l} = e^{-t_{rt}/t_c} =$$

$$= e^{-2L/vt_c}$$

we obtain:

$$t_c = L_{dye}/\alpha lv$$

introducing:

$\beta = g_f 1/\alpha 1$

we had from eq. (58):

$g_f = \ln T_{max}/T_{min}$

Therefore the field equation becomes:

$$dA/d\tau = -L/2t_c\Delta L \left(A - \int Qxdx - \beta F\right) \qquad (63)$$

and our set of normalized equations transforms into:

$$dD/\delta t = -1/\tau_2[(1+\tau_2/2\tau_1)D+(1-\tau_2/2\tau_2)M+2QAx-P(\tau)x^2] \qquad (60\text{-a})'$$

$$dM/\delta t = -1/\tau_2(\tau_2/2\tau_1 D+\tau_2/2\tau_1 M-P(\tau)x^2) \qquad (60\text{-b})'$$

$$dQ/\delta t = -(Q - ADx) / T_s \qquad (60\text{-c})'$$

$$dF/\delta t = -(F - A) / T_f \qquad (60\text{-d})'$$

$$dA/\delta z = -L/2t_c\Delta L \left(A - \int Qxdx - \beta F\right) \qquad (60\text{-e})'$$

In our modelling, we have used a Gaussian pump function in the form:

$$P(\tau) = P_0 \, 2/\Delta\tau \, [(\ln 2)/\pi]^{1/2} \exp[-(2\tau/\Delta\tau)^2 \ln 2]$$
$$= P_0 \, f(\tau) \qquad (84)$$

where $f(\tau)$ is normalized so that:

$$\int f(\tau) d\tau = 1 \qquad (85)$$

Defining the threshold parameter r as:

$$r = P/P_{th} = 1/A \left(\int Q x dx - \beta \right) \qquad (87)$$

we can determine P_0 by setting 2QAx equal to zero in eq. (80-a) and solve for the value of r in eq. (87) from the set of equations 80(a-d) and (83).

SUMMARY

In this chapter we have developed, a theoretical set of equations that describe a synchronously pumped mode-locked dye laser system with a bandwidth limiting element. The inclusion of the bandwidth tuning effects which have added a new equation, eq. (80-d), and the coupling terms in eq. (83). In the next chapter we will show the theoretical solutions and the

parameters that we used, together with the description of the experimental results that verify our theory.

Figure 3 shows a sample theoretical solution plot of: Pump function which represents P in the equations, Gain which represents D (population difference), Intensity of the dye output pulse which represents A^2, and the auto-correlation of the output pulse intensity.

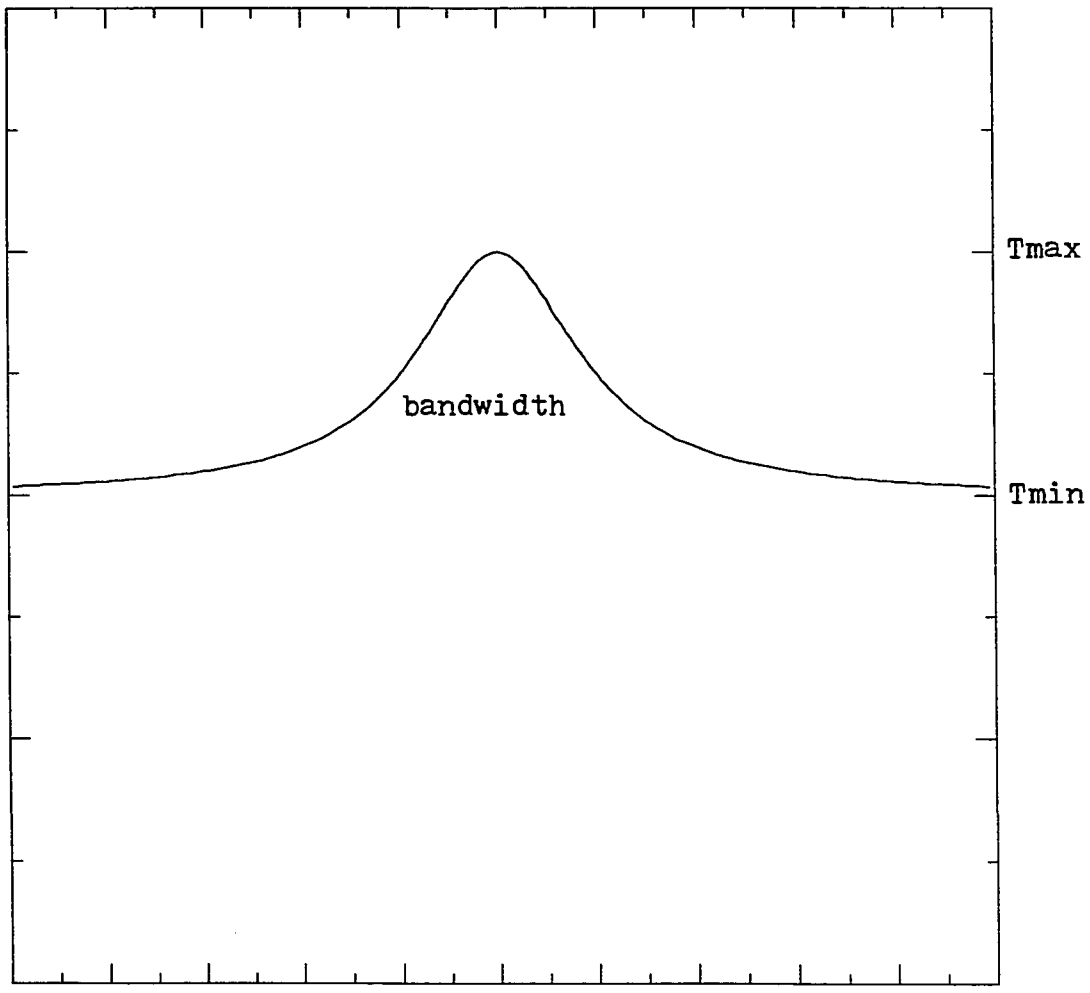

Figure 2. Lorentzian line shape.

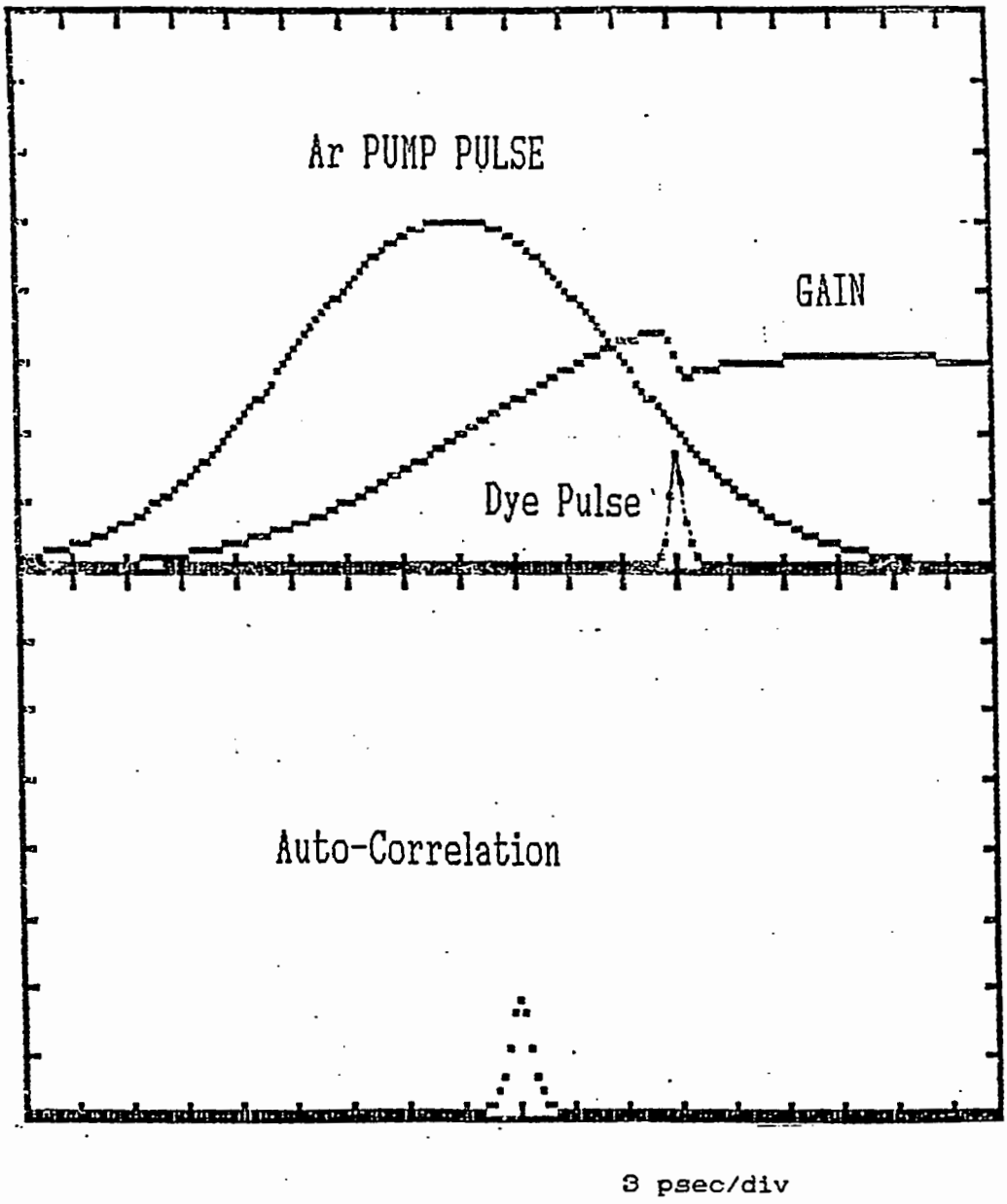

Figure 3. Sample theoretical plot.

CHAPTER III

EXPERIMENT

In order to verify the theoretical model, we designed a series of experiments. In these experiments, an acousto-optically mode-locked argon ion laser (Spectra-Physics Series 2000) was used to synchronously pump a rhodamine 6G dye laser (Spectra-Physics model 375B). To study the tuning effects, we have used two and three plate birefringent filters and a tuning wedge. The autocorrelated pulses have been measured as a function of the length detuning using a Spectra-Physics Model 409 Scanning Autocorrelator.

Figure 4 shows the general schematic of a synchronously pumped mode-locked system. It involves two lasers. The first laser, used to pump the amplifier medium of the second laser, is a mode-locked laser generating a continuous train of pulses at repetition rate $c/2L_1$, where L_1 is the optical length of the first laser's resonator. The second laser, with a resonator optical length L_2, uses an amplifier medium characterized by a recovery time shorter than the time interval $2L_1/c$ existing between two consecutive pulses of the pump laser. Under the pump excitation, the gain of the second laser is then modulated at the frequency $c/2L_1$. The

second laser will operate in a mode-locking regime, if its intermode spacing, $c/2L_2$, is adjusted to the frequency of the gain modulation, $c/2L_1$. This condition can be achieved by forcing the length of the two laser cavities to be equal.

ARGON LASER PUMP

The dye laser is pumped by the argon laser described in this section. The Spectra Physics 2020 Argon Ion laser is a high current plasma device that emits radiation at 514.5 nm. It is actively mode-locked and produces an 80 MHz train of 100 psec. pulses.

In order to have a travelling packet of light circulating inside the cavity of the argon laser, we need to force the longitudinal cavity modes of the laser to maintain a fixed relationship with each other. This process is called mode-locking and it is produced by modulating the cavity losses at a frequency equal to the frequency difference between adjacent longitudinal modes. The mode separation frequency $\Delta\nu$ is:

$$\Delta\nu = c/2L$$

where c is the speed of light, ν is the frequency and L is the laser cavity optical length. We produce the loss modulation by an acousto-optic modulator.

The index of refraction of a material changes periodically if a sound wave is passed through it. This is caused because of the change in density of the material when a sound wave is passed inside it. In our setup the sound waves are produced by a piezoelectric transducer which converts electrical signals into acoustic energy. Once the sound passes through the material, the index of refraction will change periodically. Now if a light beam also passes through the same material, it will be partially diffracted off this periodic refractive grating. The laser initially has a given amount of energy travelling within its tube. On each pass through the mode-locker, that portion of the energy arriving when the modulation function is at a minimum will be transmitted through the mode-locker. Energy arriving before or after that time will be attenuated. After several passes, the energy in the laser is in the form of a pulse which is in synchronization with the mode-locker. We measured Ar pulsewidth of 80 ps with the average power of 450 mw and modulating frequency of 40.9120 MHz.

THE SYNCHRONOUSLY PUMPED DYE LASER

We used the Spectra-Physics Model 375B dye laser system for our experiments. It consists of a three mirror resonator (Figure 5) [31], i.e. two spherical reflecting confocal mirrors and a third exit mirror; and a jet of the

organic dye in a solvent with high viscosity (ethylene glycol). The pump radiation is focused in the dye jet by a short-focus lens; synchronous operation is achieved by plane-parallel displacement of the exit mirror to match the lengths of the dye and the pump lasers.

The organic dye used in our setup was Rhodamine 6G which its energy levels was shown in Figure 1 and discussed in chapter II.

EFFECTS OF LENGTH DETUNING

The round trip time of the dye pulse within the dye optical resonator is fixed by the repetition rate of the pump pulse. The resulting length matching between the two laser cavities is then rather critical. To some degree, pulse reshaping in the amplifier medium can automatically compensate for small induced changes in the round trip propagation time, thus length mismatches on the order of 100 microns can be tolerated without destroying stable operation in the system.

This reshaping process can be qualitatively explained by considering the saturation of the gain induced by the dye pulse in the amplifier medium. Before the pulse arrival, the gain is unsaturated. Thus, the leading edge of the pulse experiences a larger gain than the trailing edge. This preferential amplification of the leading edge of the

pulse produces a new pulse that is slightly advanced, so the transit time of the pulse across the amplifier medium is shortened. The advance experienced by the dye pulse in the amplifier medium is directly related to the value of the unsaturated gain at the crossing time and occurs regardless of the laser cavity length permitting a stable operation. In particular, this reshaping effect explains the slight positive length mismatch ($L_2 = L_1 + e$) that characterizes the best modelocking operation in synchronously pumped systems.

If we shorten the dye laser cavity slightly from its optimum length, the dye pulse circulating within the optical resonator will arrive at the amplifier medium earlier than would be optimum. Since the value of the unsaturated gain is proportional to the integral of the pump pulse over time, the leading edge of the dye pulse experiences lower gain than in the optimum position. The corresponding decrease in the efficiency of the reshaping process produces an increase in the effective transit time, which can then permit continued stable modelocking of the dye amplifier.

If we lengthen the laser cavity, the dye pulse is retarded by the longer cavity and arrives at the dye later than optimum. But it *sees* higher unsaturated gain than optimum, so its transit time through the amplifier medium is reduced accordingly. Thus slight changes of the dye laser cavity during stable operation induce a readjustment of the

dye pulse shape. Lengthening the cavity retards the dye pulse, moving it further out in the gain curve past the point where the gain curve and loss line intersect. Because of the larger value of the unsaturated gain, the peak intensity of the pulse increases. At the same time, the pulse broadens to match the cavity round trip time with the period of the pump pulse. After reaching a maximum, the peak intensity of the pulse decreases for large cavity detuning (greater than 50 μm) because of the loss of unsaturated gain by spontaneous emission. Increasing the cavity length ultimately precludes complete modelocking; the characteristic "Prussian helmet" shape of the autocorrelation traces appears in the dye pulse.

If the laser cavity is shortened from the optimum position, the dye pulse moves closer to the point where the gain crosses the loss line. The peak intensity of the pulse decreases because of the lower net gain experienced, and the pulse duration slightly decreases to fulfill the pump laser timing requirements. If the gain depletion induced by the dye pulse occurs early enough, the amplifier medium (which continuely integrates the pump pulse) can recover enough gain to overcome the cavity losses. This gain recovery allows the formation of a second pulse in the laser cavity, delayed by several tens of picoseconds from the main pulse. Further length reduction decreases the delay between the two pulses and can even lead to the generation of a third or

fourth pulse in the laser cavity. If the laser cavity is shortened until the dye pulse arrives before the gain curve crosses the loss line, the pulse is quenched. Lasing continues, however, in the form of a broadband pulse whose parameters are determined by the pump pulse and the saturation characteristics of the gain medium. The mechanism of formation of short pulses is described in Appendix A.

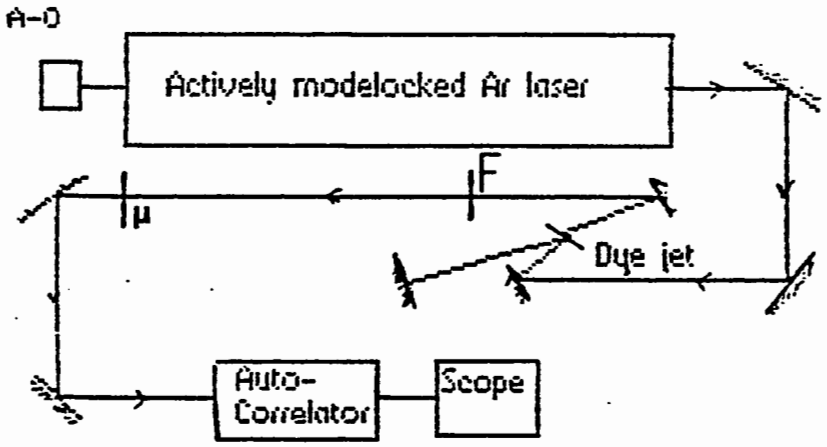

Figure 4. Our sync. pumped modelocked dye laser system.

BANDWIDTH LIMITING TUNING ELEMENTS

To isolate a wavelength of interest we used a tuning wedge and two different birefringent filters. The description of these tuning elements are as follows.

Tuning Wedge

A tuning wedge consists of a fused-silica substrate and two mirror coatings that are separated by a thickness gradient as in Figure 6 [31]. Sliding the wedge across the beam path changes the distance that light travels between the mirrored surfaces and, with it, the transmission frequency. By moving the wedge in a direction perpendicular to the cavity axis, the peak transmission of the filter is tuned to a different wavelength. The reduced loss at the new wavelength admits stimulated emission there. A tuning wedge reduces the dye laser output linewidth to about 240 GHz. We measured the bandwidth of the tuning wedge to be 25 THz as shown in Figure 10.

Birefringent Filter (Lyot) [27,28]

A birefringent filter consists of several quartz waveplates of different thicknesses (Figure 7) [32]. These plates are placed in the laser cavity at the Brewster angle such that the vertically polarized light in the cavity

experiences no loss by reflection at the plate surfaces. The no-loss condition permits amplification of light in the cavity with a high degree of linear polarization. The crystal axes of the quartz are oriented such that the plate behaves as a full waveplate for vertically polarized light if λ_0, the wavelength in a vacuum, satisfies the relation:

$$d(n_{slow} - n_{fast}) = m\lambda_0$$

where d is the thickness of the plate and m is an integer. For other wavelengths, transmission of the vertically polarized light through the plate results in elliptical polarization. After reflection at an end mirror, this elliptically polarized light experiences loss by reflection at the next encounter with the waveplate surface. This loss prevents lasing at wavelengths that differ much from those satisfying the fullwave condition. Tuning the laser is accomplished by rotating the plates, which are mounted on a common stage, about the normal to the plate surfaces. Because the plates are inclined to the optic axis, the rotation effectively changes the slow axis refractive index from n_{slow} to n'_{slow}, therefore changing the preferred wavelength to

$$\lambda'_0 = d(n'_{slow} - n_{fast})/m$$

Each tuning element has its advantages and disadvantages.

The wedge can be used over a broad wavelength range. Compared to the birefringent filter, it has high optical loss and low output power Since the birefringent filter is inserted at Brewster's angle, its loss is very low. However the plates need to be aligned for optimum performance within a limited wavelength range.

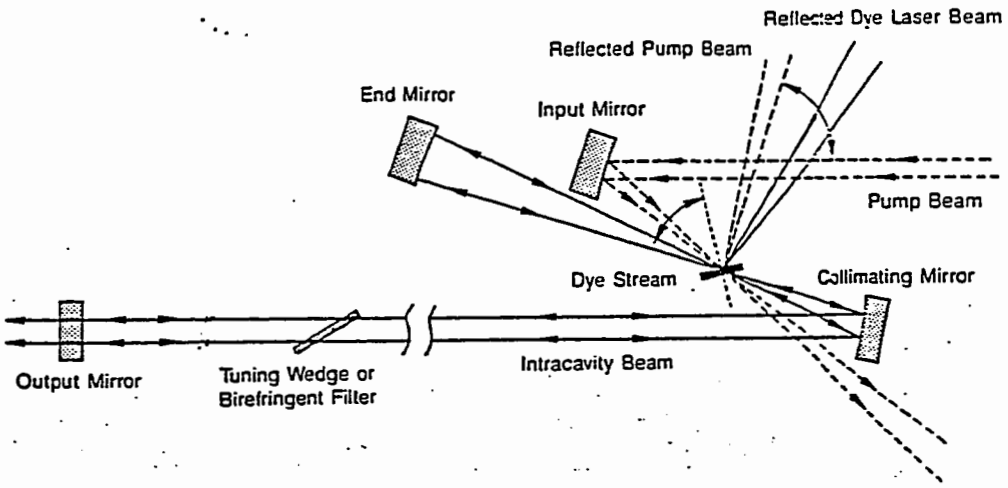

Figure 5. Dye laser closeup [31].

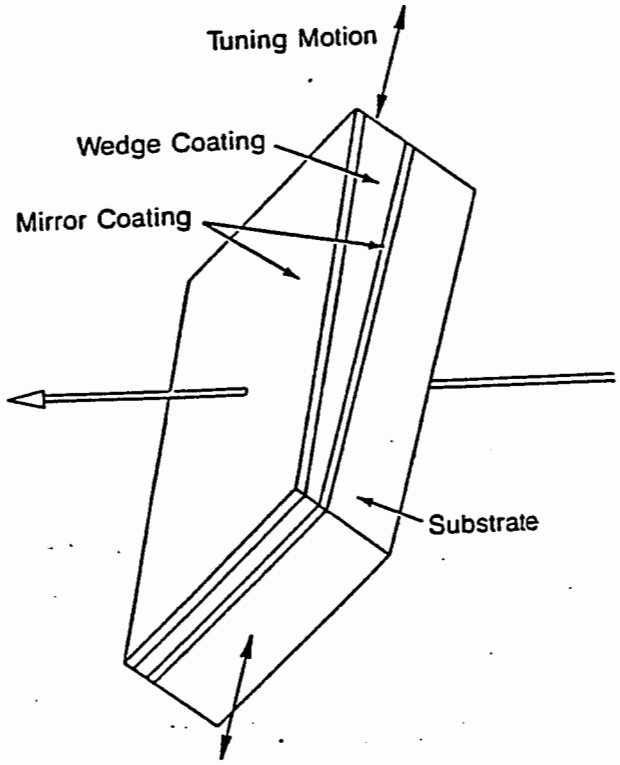

Figure 8. Tuning wedge [31].

BANDWIDTH MEASUREMENT METHODS

1. To determine the bandwidth and transmission of these filters we conducted experiments and measured the transmission vs wavelength for every filter. To measure the bandwidth of the tuning wedge, we used the Cary 14 Spectraphotometer. It consists of a white light source and a grating that would allow the white light to be differentiated into different wavelengths and a recorder that plots the transmission versus wavelength.

2. For the two birefringent filters we shined different wavelengths of light through them and measured the input and output power and therefore the transmission versus wavelength. We measured the wavelengths using a Jarrell-Ash Monospec/50 monochromator. The transmission vs wavelength curves for each of the filters are shown in Figures 8,9,10.

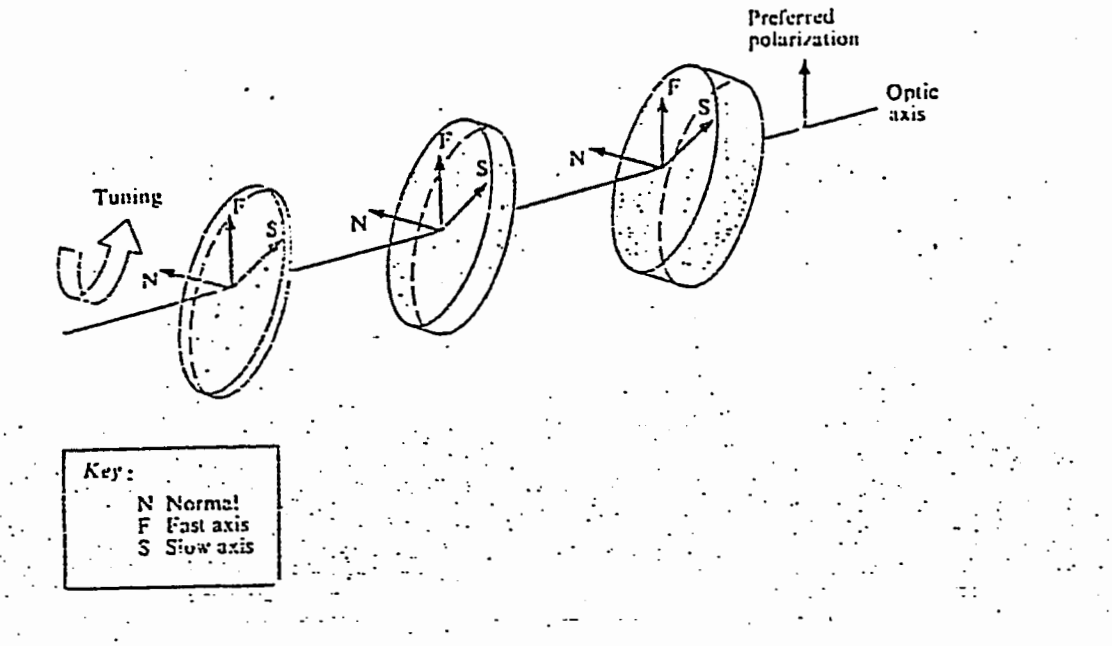

Figure 7. Birefringent filter.

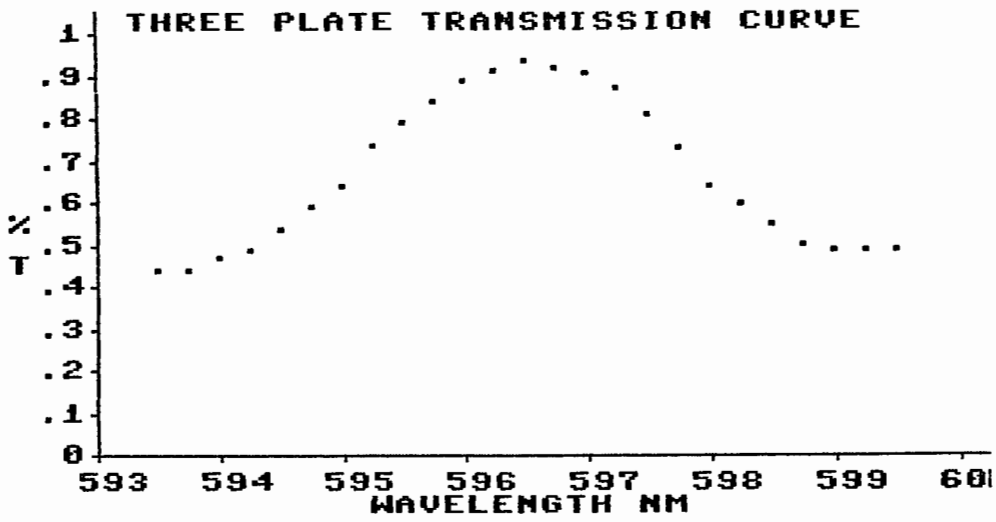

Figure 8. Three plate transmission curve.

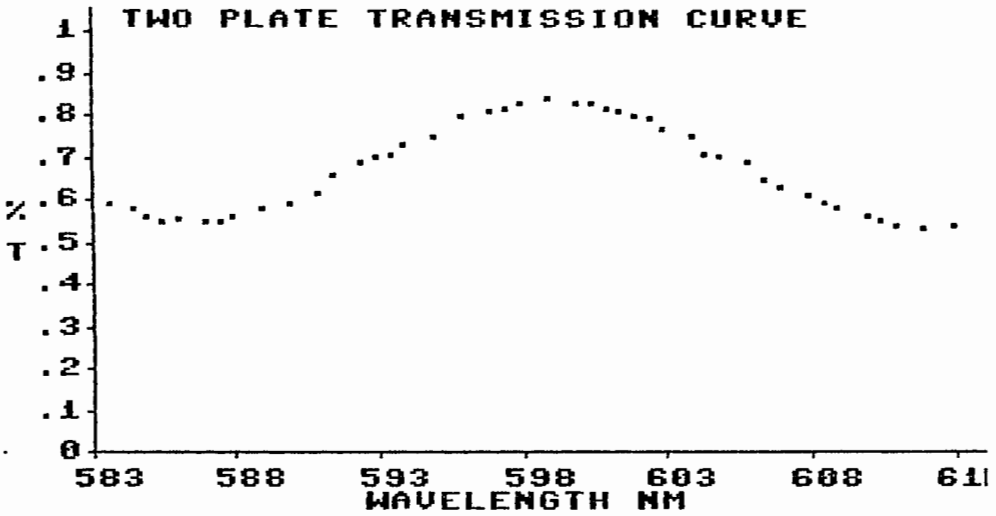

Figure 9. Two plate transmission curve.

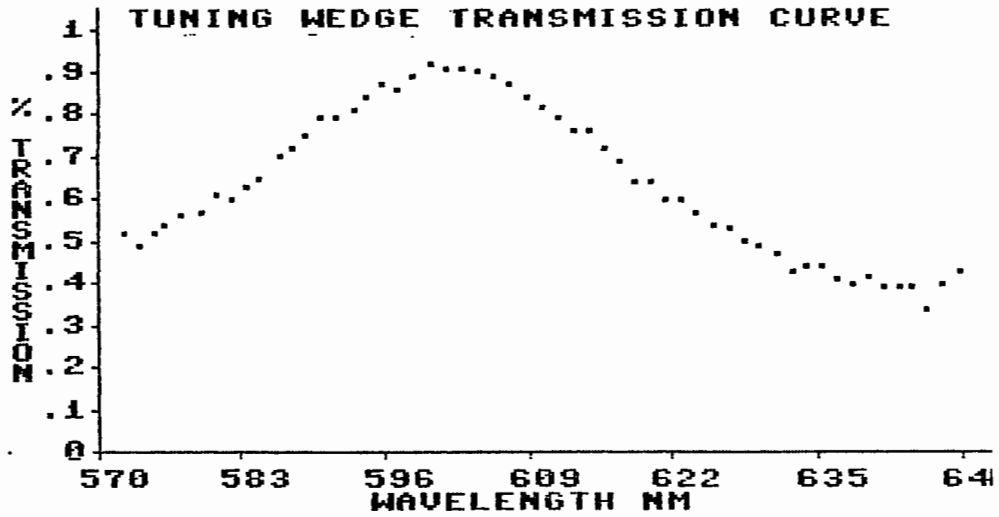

Figure 10. Tuning wedge transmission curve.

CHAPTER IV

RESULTS AND CONCLUSIONS

Figures (11,12,13,14) show the experimental autocorrelations of the output pulse shapes and the theoretical intensity autocorrelations results of our model for different filter bandwidth and length detunings. The experimental data are pictures taken from the auto-correlations of the dye laser output on a Tektronix model 7613 oscilloscope. The theoretical graphs are computer plots of the solutions of the equations.

Figures (15,16,17) the theoretical and experimental results are plotted against each other. The solid lines are the theoretical results and the experimental data points are shown by error bars. The error bars represent the range of accuracy of our data which is about %10 to %15. We notice that, the shortest pulses are produced by the widest bandwidth, as predicted by the theory. Another observation is that the pulse widths increase with length detunings.

Table I contains the parameters for our theoretical and experimental data.

TABLE I

PARAMETERS

	3 plate filter	2 plate filter	tuning wedge
bandwidth (Hz)	2.5 E 12	10.4 E 12	30 E 12
Tmax	.84	.95	.93
Tmin	.55	.12	.12
threshold parameter r	2	1.1	1
R_1 mirror reflect.	1	1	1
R_2 mirror reflect.	.93	.93	.93
τ_1	E-12	E-12	E-12
τ_2	5 E -9	5 E -9	5 E -9
T_s	5 E -14	5 E -14	5 E -14
L	1.8	1.8	1.8
t_c	2.5 E -9	13 E -9	2.5 E -9
pump pulsewidth (ps)	80	80	80
output pulsewidth (ps)	2.6	2.08	1.5

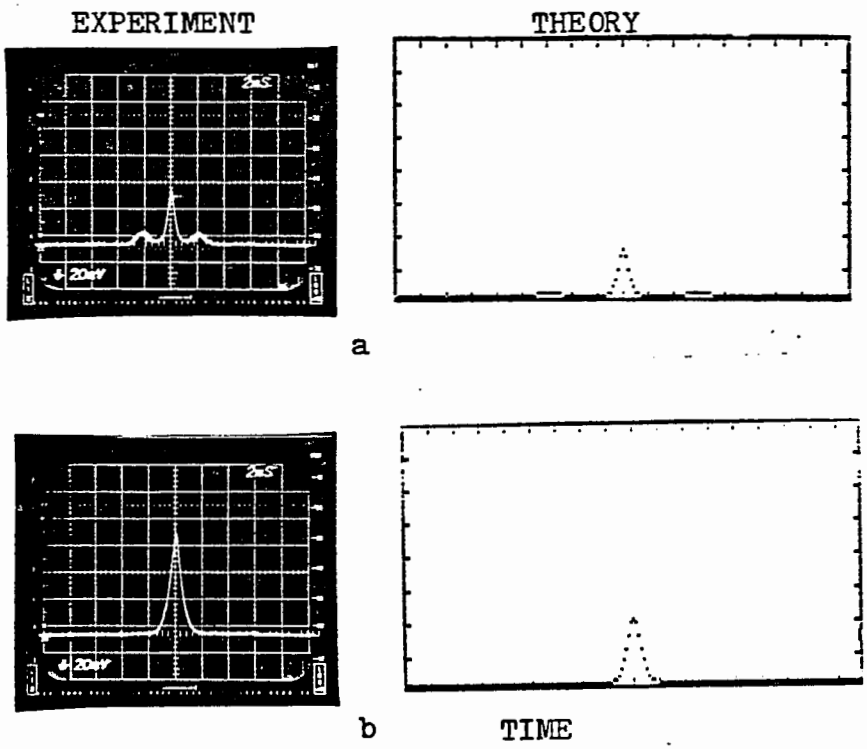

Figure 11. Autocorrelation of the output pulse for the 3 plate filter with a) 5μ and b) 18μ length detuning.

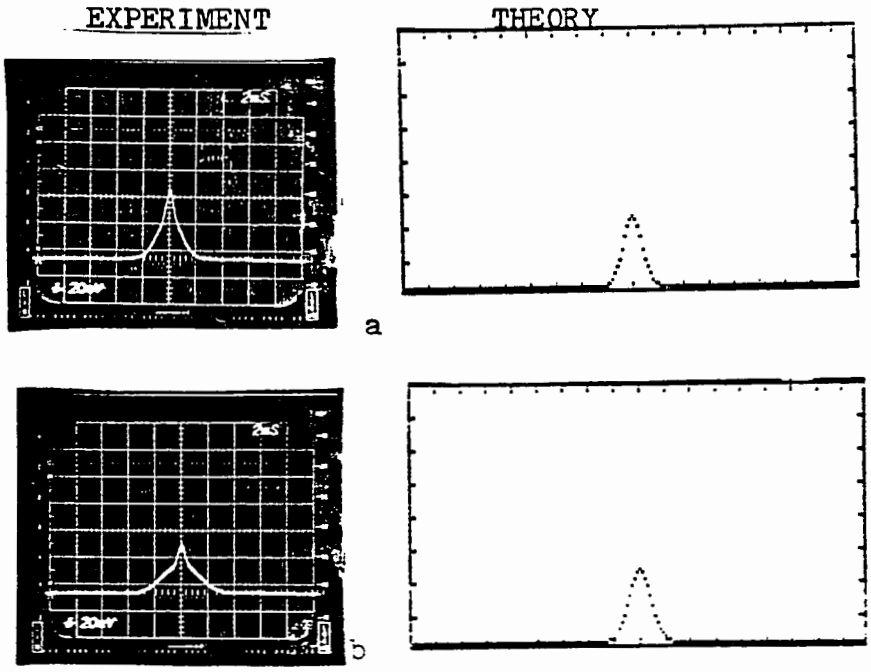

Figure 12. Autocorrelation of the output pulse for the 3 plate filter with a) 48μ and b) 71μ length detuning.

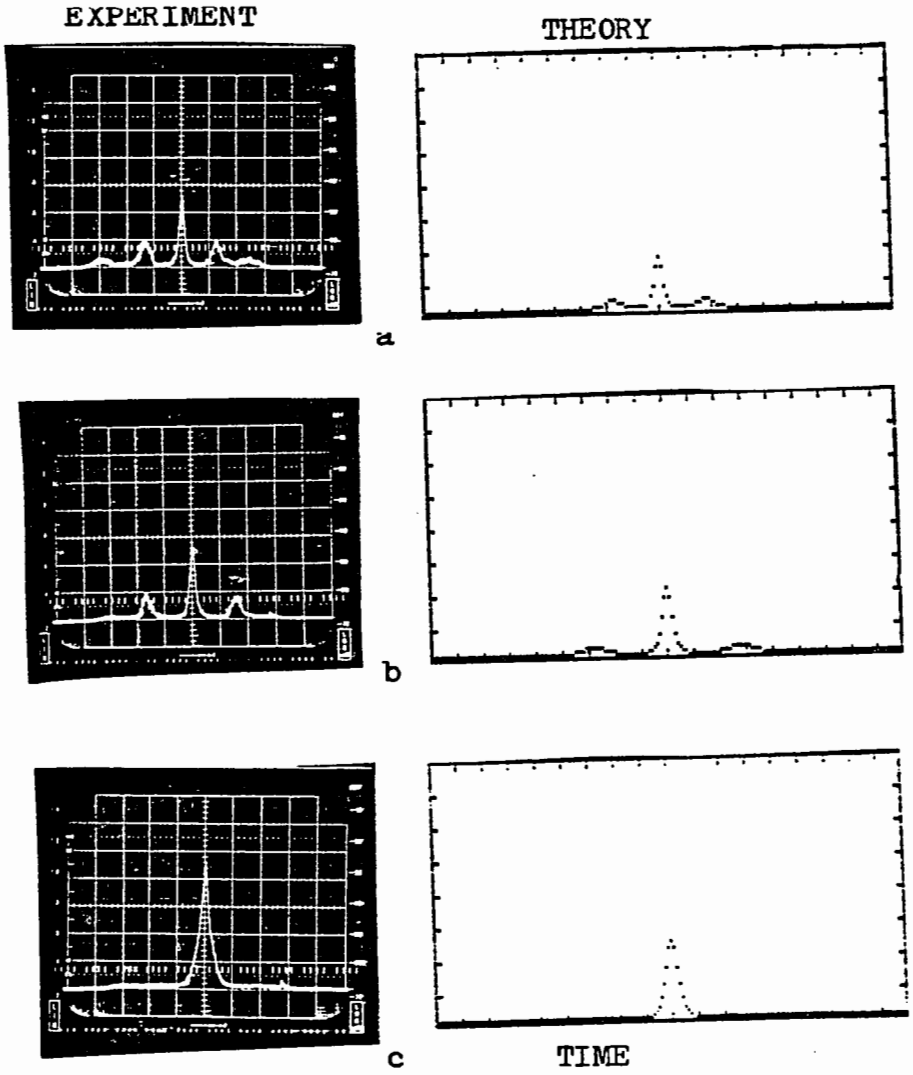

Figure 13. Autocorrelation of the output pulse for the 2 plate filter with a) 3μ, b) 6μ and c) 11μ length

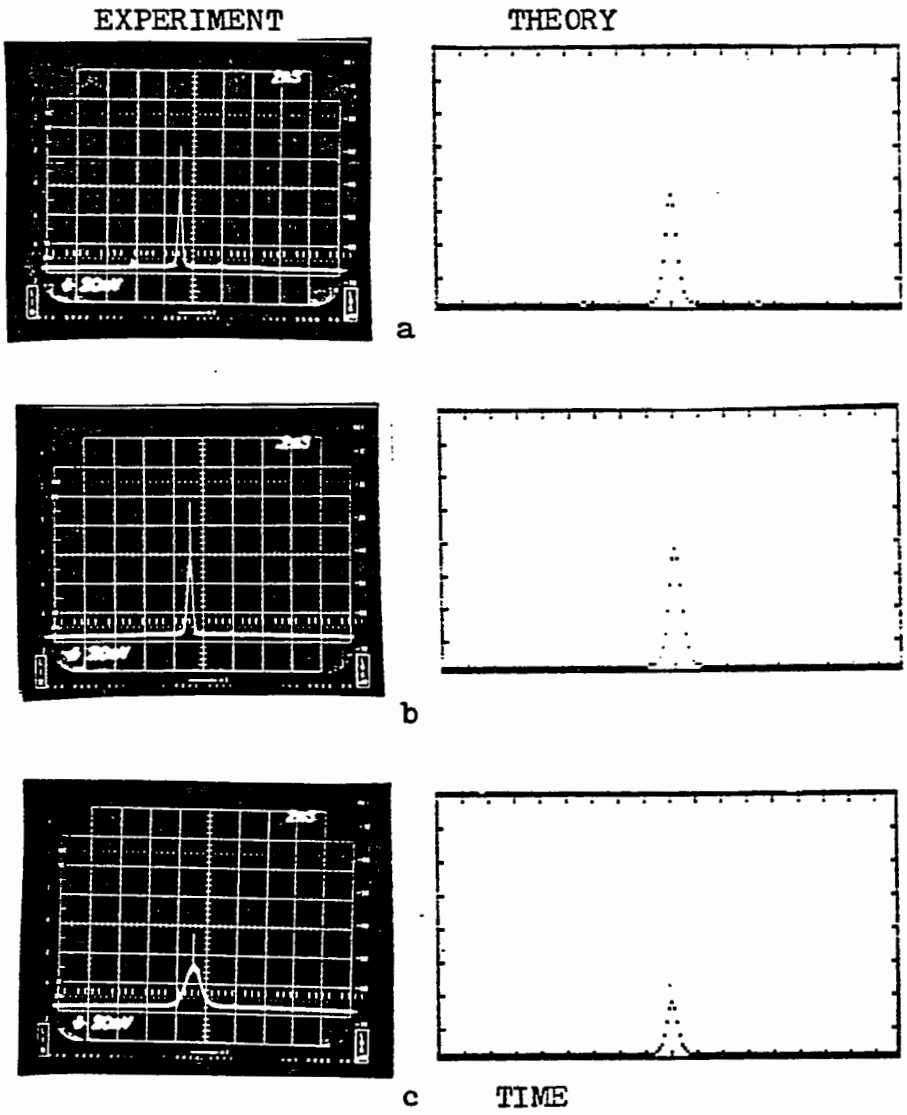

Figure 14. Autocorrelation of the output pulse for the tuning wedge with a) 2μ, b) 6μ and c)21μ length detuning.

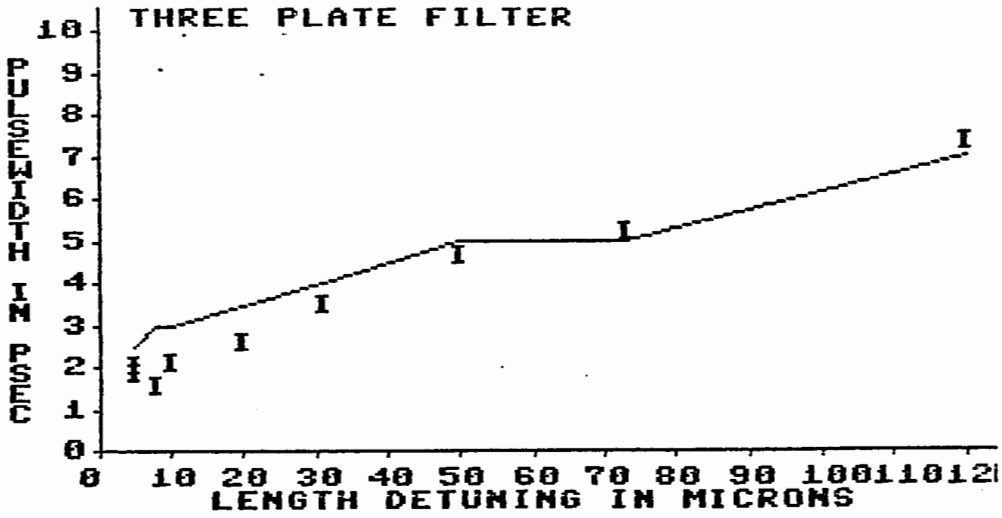

Figure 15. Theoretical line and experimental bars for the 3 plate filter.

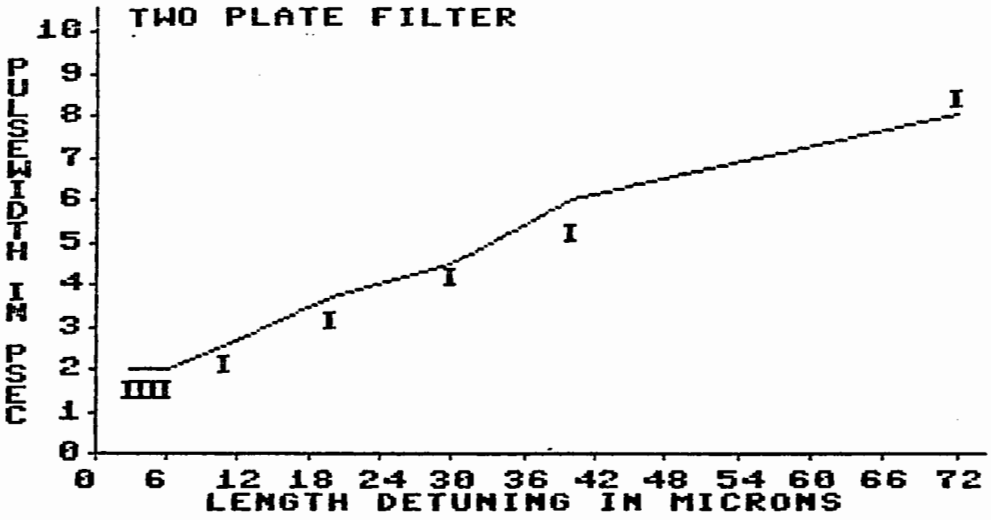

Figure 18. Theoretical line and experimental bars for the 2 plate filter.

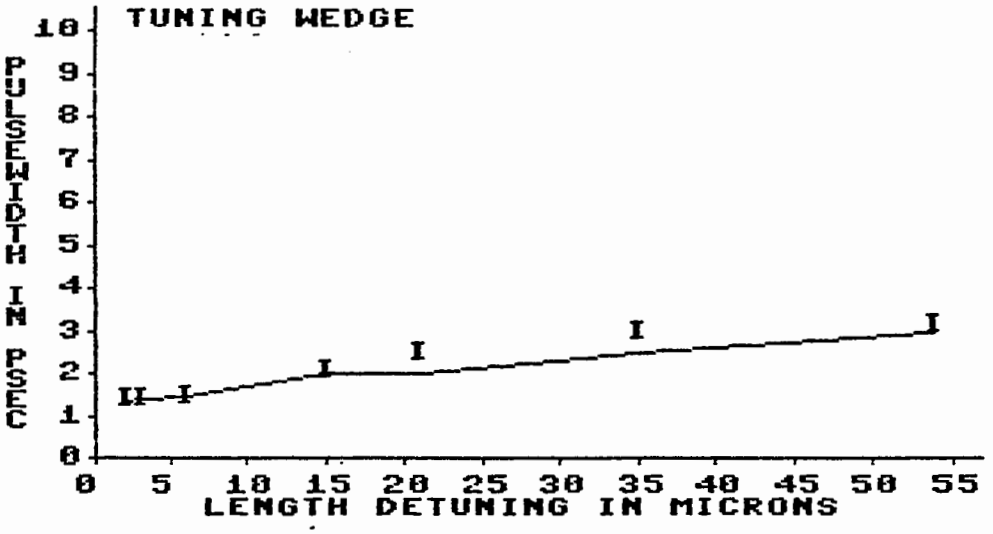

Figure 17. Theoretical line and experimental bars for the tuning wedge.

CONCLUSIONS

In this study we have experimentally verified a semi-classical model for synchronously pumped mode-locked dye lasers producing tunable picosecond pulses. An improved description of the bandwidth limiting tuning filter has been introduced within a semi-classical model. The new set of equations has been solved numerically using the best available values for the various parameters, and autocorrelations have been computed for a range of different length detuning and bandwidth limiting elements. The experimental pulse shapes agree closely with the theoretical solutions for all values of detuning and filter bandwidth. In the next chapter, through a sensitivity analysis, it is shown how this model can be used for engineering design purposes to select values for the transmission and the bandwidth of the filter to obtain optimum pulse characteristics.

CHAPTER V

FURTHER NUMERICAL STUDIES

SENSITIVITY ANALYSIS (ENGINEERING DESIGN)

Now that the theory has been verified experimentally, we can study how the theory behaves numerically on a computer. We have two different parameters for our model of the filter:

1. Bandwidth of the filter T_f.
2. The ratio [ln (Tmax/Tmin)] / losses = β

We now study the behavior of the theoretical pulse characteristics as a function of the two parameters associated with the filter. Among the various factors there are the two most pertinent:

1. The Peak Intensity I_{peak}.
2. The Pulsewidth T_{pulse}.

We study these two parameters as a function of β and T_f as shown in figures 18-21. In case of β, we have kept the sum of losses (α) constant, therefore the only parameter changing in β is T_{max}. For engineering design, these curves can be used to obtain a filter element with desired parameters. From the plots we can observe that:

a. Low β values produce high peak intensities and shorter pulses. This means lower T_{max} leads to higher peak intensities and shorter pulses.

b. Large T_f produce shorter pulses.

c. Peak intensities are insensitive to T_f.

SUGGESTIONS FOR FURTHER STUDIES

Further work can be suggested in cases which are not considered in this study. These include the following: One can study specialized filter shapes instead of our Lorentzian. Also filter detunings from the line center of the dye can be studied.

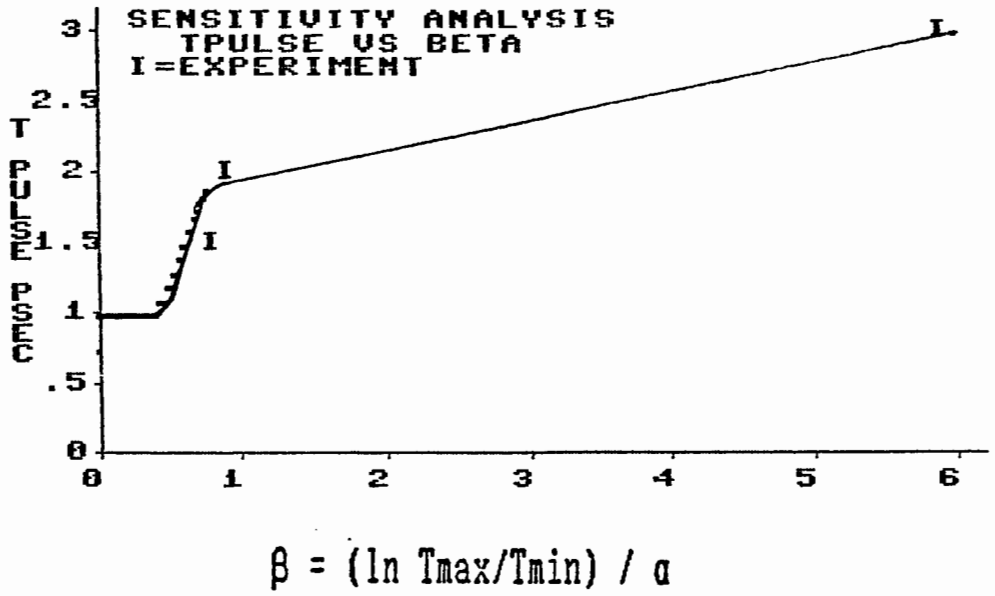

Figure 18. Pulsewidth vs β.

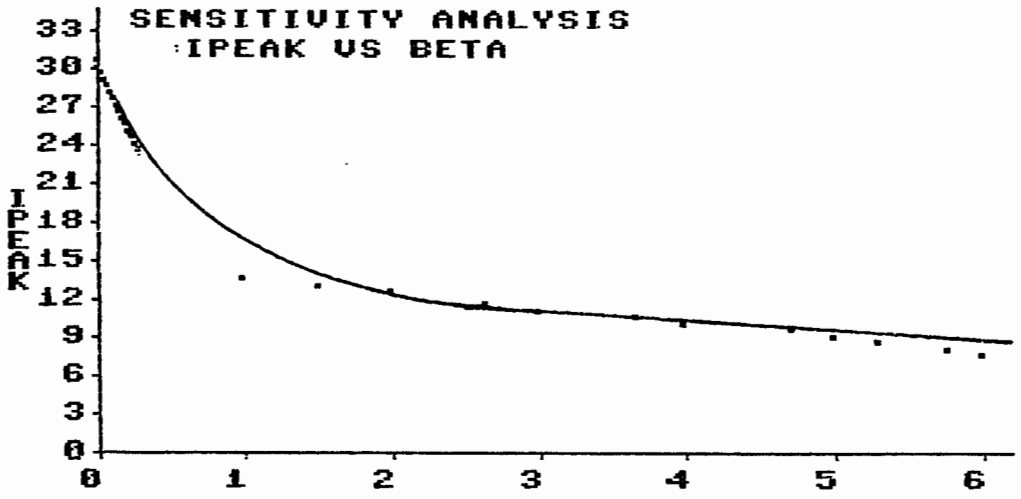

$$\beta = (\ln T_{max}/T_{min}) / \alpha$$

Figure 19. Peak intensity vs β.

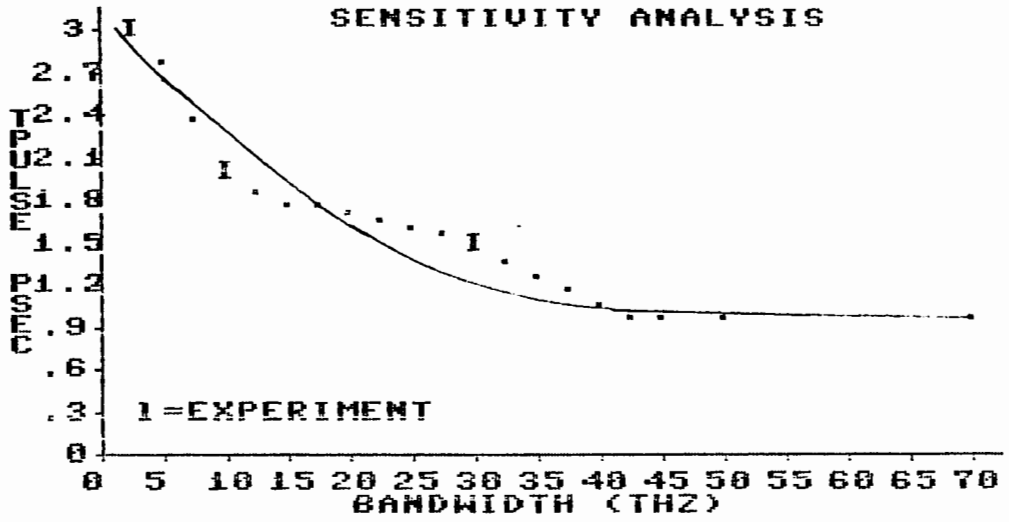

Figure 20. Pulsewidth vs bandwidth.

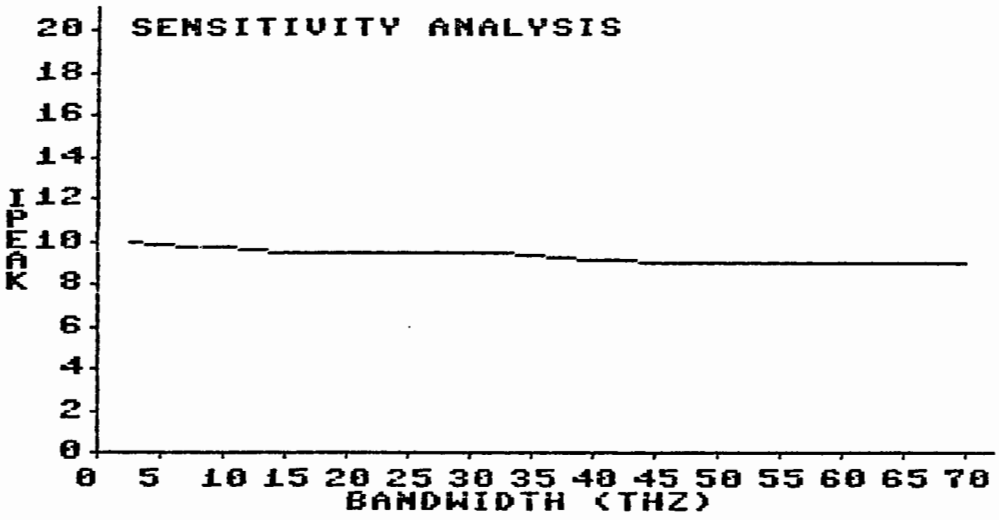

Figure 21. Peak intensity vs bandwidth.

REFERENCES CITED

[1] Z.A. Yasa and O. Teschke, Optics Communication, vol. 15, p. 169, 1975.

[2] A. Scavennec, Optics Communication, vol.17, p. 14, 1976.

[3] Z.A. Yasa, Applied Physics B, vol. 30, p. 135, 1983.

[4] G.H.C. New and J.M. Catherall, Optics Communication, vol. 50, p. 111, 1984.

[5] W. Heudorfer and G. Marowsky, Applied Physics, vol. 17, p. 181, 1978.

[6] P.G. Kryukov and V. S. Letokhov, Soviet Physics Usp., vol. 12, p. 641, 1970.

[7] D. Faubert and S.L. Chin, Canadian Journal of Physics, vol. 57, p. 1359, 1979.

[8] D.M. Kim, J. Kuhl, R. Lambrich, and D. von der Linde, Optics Communication, vol. 27, p. 123, 1978.

[9] A.E. Siegman and D.J. Kuizenga, Opto-Electronics, vol. 6, p. 43, 1974.

[10] C.P. Ausshnitt and R.K. Jain, Applied Physics Letters, vol. 32, p. 727, 1978.

[11] C.P. Ausshnitt, R.K. Jain, and J.P. Heritage, IEEE Journal of Quantum Electronics, vol.15, p. 912, 1979.

[12] H.A. Haus, IEEE Journal of Quantum Electronics, vol. 11, p. 736, 1975.

[13] H.A. Haus, IEEE Journal of Quantum Electronics, vol. 11, p. 323, 1975.

[14] H.A. Haus, Journal of Applied Physics, vol. 46, p. 3049, 1975.

[15] J. Herrmann and U. Motschmann, Optics Communication, vol. 40, p. 379, 1982.

[16] J. Herrmann and U. Motschmann, Applied Physics B, vol. 27, p. 27, 1982.

[17] L.M. Davis, J.D. Harvey, and J.M. Peart, Optics Communication, vol. 50, p. 49, 1984.

[18] D. von der Linde, D. Wiechert, and J. Kluge, et al, Proceedings of the Third International Symposium on Ultrafast Processes in Spectroscopy, Minsk, 1983.

[19] J.M. Catheral, G.H.C. New, and P.M. Radmore, Optics Letters, vol. 7, p. 319, 1982.

[20] L.W. Casperson, Journal of Applied Physics, vol. 54, p. 2198, 1983.

[21] V.A. Nekhaenko, S.M. Pershin, and A.A. Podshivalov, Soviet Journal of Quantum Electronics, vol. 16, no. 3, p. 299, 1986.

[22] H. Haken, Laser Theory, Springer Verlag, 1969.

[23] W.E. Lamb, Jr., Physical Review A, vol. 134, p. 1429, 1964.

[24] A. Yariv, Quantum Electronics, John Wiley & Sons, 1967.

[25] L.W. Casperson and A. Yariv, IEEE Journal of Quantum Electronics, vol. 8, no. 2, 1972.

[26] F.P. Schafer, Dye Lasers, Topics in Applied Physics, vol. 1, Springer Verlag, 1973.

[27] G. Holtom and O. Teschke, IEEE Journal of Quantum Electronics, vol. 10, no. 8, 1974.

[28] D.R. Preuss and J.L. Gole, Applied Optics, vol. 19, no. 5, 1980.

[29] Spectra-Physics Model 409 Scanning Autocorrelator Manual.

[30] A.J. De Maria, et al, IEEE Journal of Quantum Electronics, vol. 57, no. 1, p. 2, 1969.

[31] Spectra-Physics Model 375B Dye Laser Manual.

[32] D.C. O'Shea, W.R. Callen and W.T. Rhodes, Introduction to Lasers and Their Applications, Addison-Wesley, 1976.

APPENDIX A

MECHANISM OF FORMATION OF A PICOSECOND PULSE [21]

To study pulse-shape evolution in the dye laser with length detuning, we assume that a steady-state regime has been obtained: A narrow pulse is travelling within the dye laser's optical cavity. The oscillation conditions require that the dye pulse crosses the amplifier medium when the gain induced by the pump pulse is larger than the intracavity losses. Figure 22 gives a schematic of the variation of the gain due to the passing of the pump and dye pulses through the dye amplifier medium. The horizontal axis is in arbitrary units of time at the dye medium. At t=0, the pump pulse arrives at the amplifier medium, pumping the dye molecules to the excited state. The gain builds up following the integral of the pump pulse intensity, until the dye pulse travelling within the cavity reaches the dye amplifier. At this time, a loss of population inversion due to the stimulated emission caused by the dye pulse is induced in the medium. This loss of population shows as a sharp dip in the gain curve at exactly the same time that the dye pulse strikes the amplifier. While the gain drops below the level of the intracavity losses, the long duration of the pump pulse allows the gain to build up again after the dye pulse has passed.

Figure 22 shows the calculated evolution of the generation of ultrashort pulses. In Figure 22a, the first argon pump amplifies the dye and generates long pulses here the gain is greater than the losses. In Figure 22b, the dye amplification lowers gain and narrows the pulse. Figure 22c the amplification saturates andthe pulsewidth gets narrower and Figure 22d is the steady state where the increase in the gain due to pumping is compensated by its reduction due to amplification of the dye pulse.

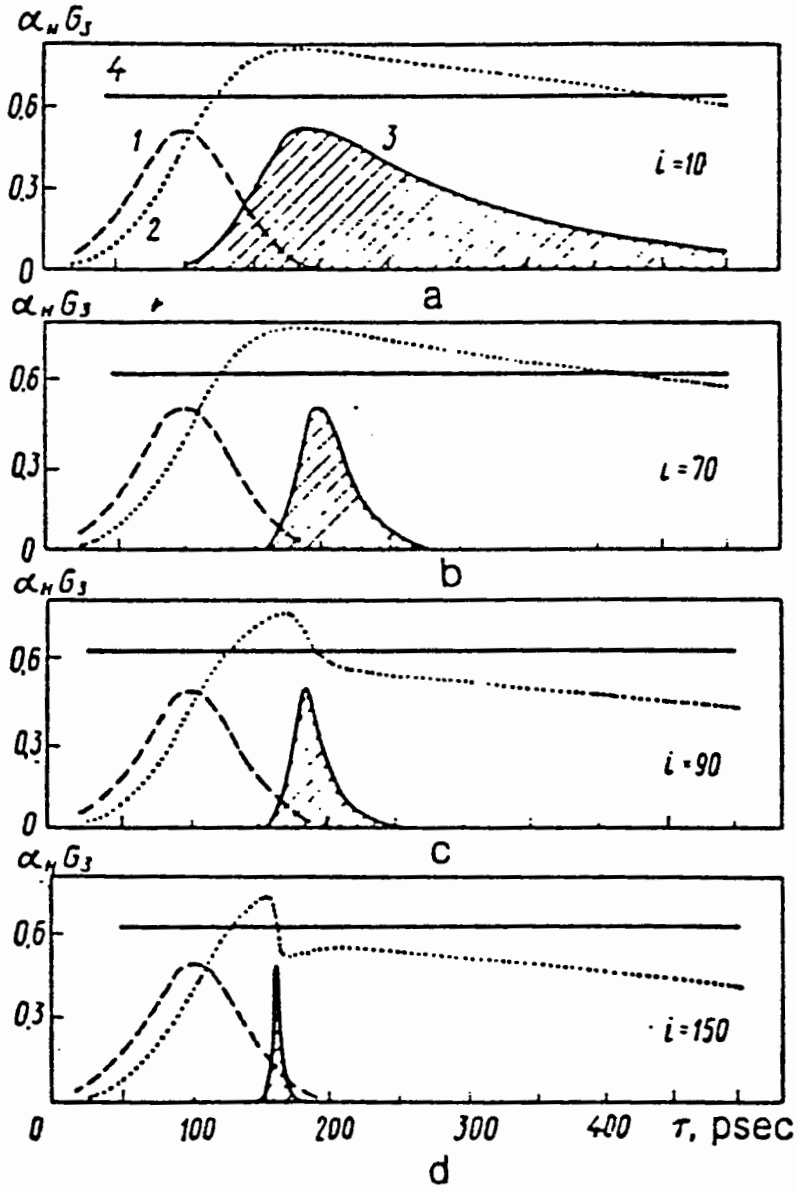

Figure 22. Short pulse formation [21].

APPENDIX B

MEASURING PICOSECOND PULSES

THE AUTOCORRELATION TECHNIQUE FOR MEASURING ULTRA-SHORT PULSES [29]

The most common method used for measuring pico-second pulse-widths is the auto-correlation technique. This technique translates differences in optical path length into time, using the fact that the speed of light is constant. An incoming pulse train is split into two beams of equal intensity. An adjusted optical delay is applied to one of the beams and the two beams are then recombined within a nonlinear crystal for second harmonic generation which is proportional to the degree of pulse overlap within the crystal. The intensity of ultraviolet generation as a function of delay between the recombining pulses produces a correlation function related to pulse width. The Spectra-Physics Model 409 Scanning Autocorrelator operates in a background-free configuration in which the two beams are displaced from a common optical axis and recombined in a noncollinear fashion as in figure 28. In this configuration, the background is eliminated because ultraviolet is generated only at the point where the two beams intersect with correct phase

matching conditions.

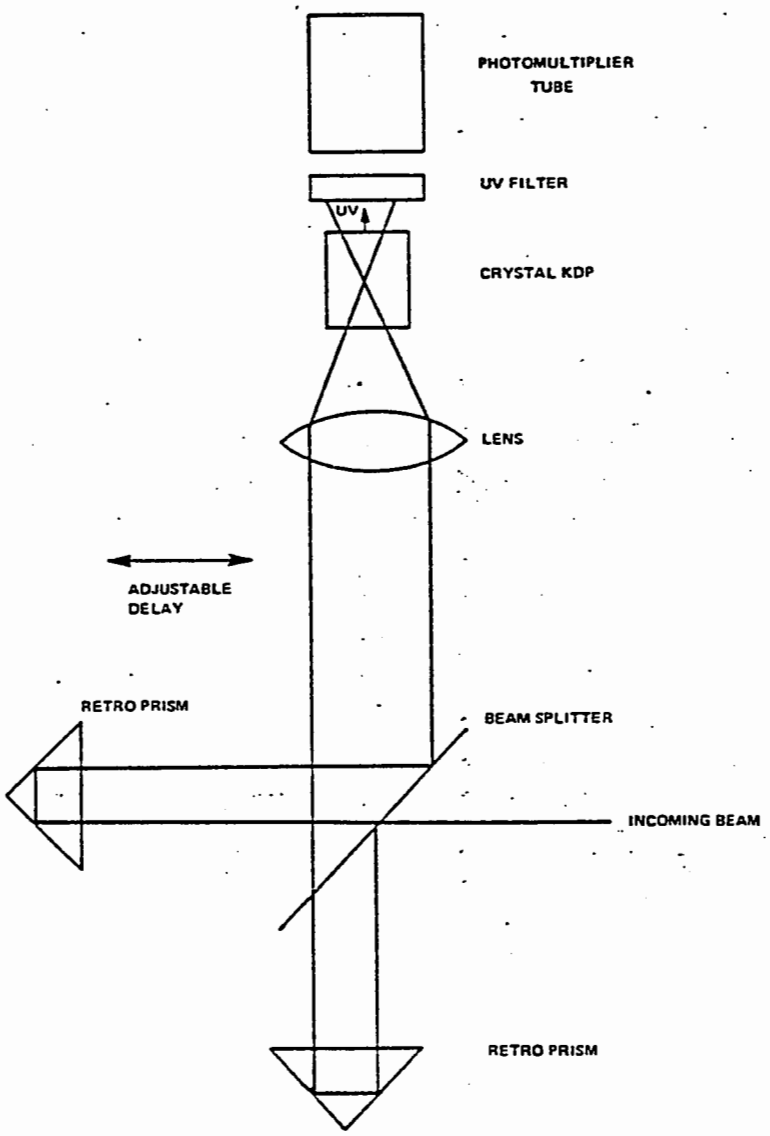

Figure 23. Schematic of Spectra-Physics model 409 autocorrelator [29].